Skin-specific Deletion of Stearoyl-CoA Desaturase-1 Alters Skin Lipid Composition and Protects Mice from High Fat Diet-induced Obesity*[S]

Harini Sampath[‡1], **Matthew T. Flowers**[§], **Xueqing Liu**[§], **Chad M. Paton**[§], **Ruth Sullivan**[¶], **Kiki Chu**[§], **Minghui Zhao**[§], **and James M. Ntambi**[‡§2]

From the Departments of [‡]Nutritional Sciences and [§]Biochemistry and the [¶]Research Animal Resources Center, University of Wisconsin, Madison, Wisconsin 53706

Stearoyl-CoA desaturase-1 (SCD1) catalyzes the synthesis of monounsaturated fatty acids and is an important regulator of whole body energy homeostasis. Severe cutaneous changes in mice globally deficient in SCD1 also indicate a role for SCD1 in maintaining skin lipids. We have generated mice with a skin-specific deletion of SCD1 (SKO) and report here that SKO mice display marked sebaceous gland hypoplasia and depletion of sebaceous lipids. In addition, SKO mice have significantly increased energy expenditure and are protected from high fat diet-induced obesity, thereby recapitulating the hypermetabolic phenotype of global SCD1 deficiency. Genes of fat oxidation, lipolysis, and thermogenesis, including uncoupling proteins and peroxisome proliferator-activated receptor-γ co-activator-1α, are up-regulated in peripheral tissues of SKO mice. However, unlike mice globally deficient in SCD1, SKO mice have an intact hepatic lipogenic response to acute high carbohydrate feeding. Despite increased basal thermogenesis, SKO mice display severe cold intolerance because of rapid depletion of fuel substrates, including hepatic glycogen, to maintain core body temperature. These data collectively indicate that SKO mice have increased cold perception because of loss of insulating factors in the skin. This results in up-regulation of thermogenic processes for temperature maintenance at the expense of fuel economy, illustrating cross-talk between the skin and peripheral tissues in maintaining energy homeostasis.

Obesity is a multifactorial disease stemming from a combination of genetic, dietary, and lifestyle factors and the interaction between these components (1–3). The microsomal enzyme, stearoyl-CoA desaturase-1 (SCD1),[3] is a critical con-trol point in the development of metabolic diseases, including obesity and insulin resistance. SCD1 catalyzes the conversion of saturated fatty acids, such as palmitate (16:0) and stearate (18:0), into their Δ-9 monounsaturated products, palmitoleate (16:1 *n*-7) and oleate (18:1 *n*-9), respectively. Mice lacking the SCD1 enzyme because of a global deletion of the *Scd1* gene (GKO) are lean and protected from diet-induced and leptin deficiency-induced obesity. These mice have a marked increase in energy expenditure and almost complete protection from high fat diet-induced weight gain and glucose intolerance (4–10).

Because SCD1 is expressed in multiple tissues, including liver, brown and white adipose tissue, skeletal muscle, and skin, it has been difficult to determine the relative contributions of these tissues to the dramatically altered metabolic phenotypes of GKO mice. Studies using antisense oligonucleotide-mediated approaches to knock down *Scd1* expression have reported protection from diet-induced weight gain and hepatic insulin resistance upon hepatic SCD1 inhibition (11–13). However, whereas the liver is a major target of these antisense oligonucleotides, they have also been reported to affect expression of target genes in adipose tissue (13, 14) and possibly other organs (15). Using Cre recombinase-mediated inhibition of hepatic *Scd1*, we recently reported that chronic deletion of SCD1 specifically in liver does not protect mice from high fat diet-induced obesity (16), suggesting that extra-hepatic tissues may play a more prominent role in the increased energy expenditure phenotype of global SCD1 deficiency (16).

In addition to their hypermetabolic phenotype, global SCD1 deficiency also elicits marked cutaneous phenotypes, including dry skin, alopecia, and sebocyte hypoplasia (7, 17, 18). Given the severity of this skin phenotype in GKO mice, we sought to establish a specific role for SCD1 in the skin. In this study, we used the Cre-lox system to generate mice with a skin-specific deletion of SCD1 (SKO). We report here that SKO mice have a severe paucity of lipid-enriched sebocytes in the skin, resulting in dry skin, alopecia, and marked alterations in levels of key skin lipids. Unlike mice with global or liver-specific deletion of SCD1 (7, 16), SKO have an intact hepatic lipogenic response to dietary stimuli. However, deletion of skin SCD1 completely

[1] Present address: Center for Study of Weight Regulation and Associated Disorders, Oregon Health and Science University, Portland, OR 97239.

[2] To whom correspondence should be addressed: University of Wisconsin-Madison, 433 Babcock Dr., Madison, WI 53706. Tel.: 608-265-3700; Fax: 608-265-3272; E-mail: ntambi@biochem.wisc.edu.

[3] The abbreviations used are: SCD1, stearoyl-CoA desaturase-1; BAT, brown adipose tissue; CE, cholesterol ester; GKO, global SCD1-knockout; PPAR, peroxisome proliferator-activated receptor; SREBP, sterol regulatory element-binding protein; SKO, skin-specific SCD1-knockout; T₃, triiodothyro-nine; UCP, uncoupling protein; WAT, white adipose tissue; WDE, wax diesters; TG, triglyceride; MUFA, monounsaturated fat; HFD, high fat diet; FC, free cholesterol.

recapitulates the increased energy expenditure phenotype of GKO mice (7) and protects SKO mice from high fat diet-induced obesity, hepatic steatosis, and glucose intolerance. Elevation of genes encoding for cold-inducible factors, including peroxisome proliferator-activated receptor γ co-activator-1α (*Pgc-1α*) and uncoupling proteins (*Ucps*) in brown and white adipose tissue and skeletal muscle of SKO mice, suggests up-regulation of thermogenic processes for maintenance of core body temperature in SKO mice. Furthermore, the hypermetabolic phenotype of SKO mice, coupled with the loss of insulating factors in the skin, results in severe cold intolerance in SKO mice that is ameliorated by prior feeding with a high fat diet. To the best of our knowledge, this study represents the first example of skin-specific deletion of a lipogenic enzyme resulting in profound changes in systemic energy metabolism. These data elucidate an as yet under-appreciated role for skin SCD1 in triggering the altered metabolic phenotypes caused by global SCD1 deletion.

MATERIALS AND METHODS

Animals and Diets—The generation of mice having the third exon of the *Scd1* gene flanked by loxP sites (Scd1$^{flox/flox}$) has been described previously (16). To generate skin-specific Scd1 knock-out mice, female Scd1$^{flox/flox}$ mice were crossed with Keratin-14 Cre mice (K14-Cre; mixed Swiss Webster; C57Bl/6J; CBA/J; The Jackson Laboratory, Bar Harbor, ME) (19) that were fully backcrossed onto the C57Bl/6J background to generate compound heterozygous (Scd1$^{flox/+;Cre/+}$) mice. Male Scd1$^{flox/+;Cre/+}$ mice were subsequently mated with female Scd1$^{flox/flox}$ (Lox) mice, generating Scd1$^{flox/flox;Cre/+}$ mice (SKO). For litter expansion, male SKO mice were bred with female Lox mice. All mice were on a fully backcrossed C57Bl/6J background, and Lox and SKO mice were born in an expected ratio of 1:1. Genotyping was performed by PCR using genomic DNA isolated from a tail clip, as described previously (16). Mice were maintained on a 12-h light/dark cycle with free access to water and either a standard chow diet (Purina 5008) or special formulations as indicated. Detailed diet formulations and feeding conditions are presented in the supplemental Methods. All animals were sacrificed by isoflurane overdose without fasting, unless otherwise indicated, and tissues and plasma were rapidly removed, snap-frozen in liquid nitrogen, and stored at -80 °C. For preparation of nuclear protein, fresh liver was homogenized immediately upon excision. All *in vivo* experimental procedures were approved by the Animal Care Research Committee of the University of Wisconsin-Madison.

Cold Tolerance Tests—Cold tolerance tests were performed as described previously (20) in 12-week-old male and female Lox and SKO mice that were individually caged and allowed *ad libitum* access to food and water.

Histology—Fresh liver, white adipose, and skin samples from similar sites in age- and gender-matched Lox and SKO mice were fixed in 10% buffered formalin and paraffin-embedded for sectioning and staining with hematoxylin and eosin. For Oil Red O staining of skin samples, frozen skin samples were embedded in cryosectioning medium prior to sectioning and staining.

Energy Expenditure—Energy balance was assessed using the PhysioScan Oxygen Consumption/Carbon Dioxide Production System (AccuScan Instruments Inc.) at the University of Cincinnati Mouse Metabolic Phenotyping Center. 12-Week-old male mice were placed in the PhysioScan chamber with food 3 h before the dark cycle, and energy expenditure was measured for the next 48 h, as described previously (21). VO_2 and VCO_2 values were normalized to total body weights, as there were no significant differences in body weights between the genotypes. Heat was calculated from recorded VO_2 values.

*Analytical Procedures*—Glucose tolerance tests, basal plasma glucose, and plasma insulin measurements were performed in mice fasted for 4 h as described previously (16). Hepatic glycogen was measured by an enzyme-coupled spectrophotometric assay as described previously (16). Plasma insulin was measured using an insulin radioimmunoassay, and plasma leptin was measured with a mouse leptin enzyme-linked immunosorbent assay (both from Millipore). Plasma cholesterol and TG were analyzed by colorimetric enzyme assay using the Infinity TG and cholesterol reagents (Thermo Electron). Skin free cholesterol (FC) was measured using a free cholesterol colorimetric enzyme assay (Wako). Plasma T_3 and thyroxine were measured at Analytics, Inc. (Gaithersburg, MD).

Lipid Analyses—Skin surface lipids were extracted by dipping carcasses into 100 ml of chloroform/methanol (2:1, v/v) followed by 100 ml of acetone. Lipid extracts were pooled, dried down under a stream of N_2, and resuspended in equal volumes of chloroform/methanol (2:1, v/v) for loading onto TLC plates. Hepatic lipids were extracted from 30 mg of frozen liver by the Folch method (22). Hepatic and skin lipids were separated and analyzed by TLC and gas chromatography as described previously, with penta- and heptadecanoic acids added as internal standards (17, 23, 24). Details on developing solvents are presented in supplemental Methods.

Real Time Quantitative PCR—Quantitative PCR was performed as described previously (16). Results are expressed as mean $\pm$ S.E. after normalizing to expression of a housekeeping gene (*Arbp* or cyclophilin) using the $\Delta\Delta Ct$ method. Primer sequences are available upon request.

Western Blot Analysis—Nuclear extracts (25) and microsomal fractions (26) were prepared as described for immunoblotting of SREBP and SCD1, respectively. Polyclonal anti-SREBP-1 (Pharmingen), SREBP-2 (kindly provided by Dr. Jay Horton), histone H_3 (Santa Cruz Biotechnology), or SCD1 (Santa Cruz Biotechnology) were used as primary antibodies, followed by the appropriate IgG-horseradish peroxidase-conjugated secondary antibody. Proteins were visualized by ECL.

Data and Statistical Analyses—Data are expressed as mean $\pm$ S.E. with comparisons carried out using a Student's *t* test or analysis of variance where appropriate, using the program GraphPad Prism. When a significant *F* ratio was obtained (significance $p < 0.05$), post-hoc analysis was conducted between groups using a multiple comparison procedure with Bonferroni/Dunn post-hoc comparison. p values < 0.05 were considered significant.
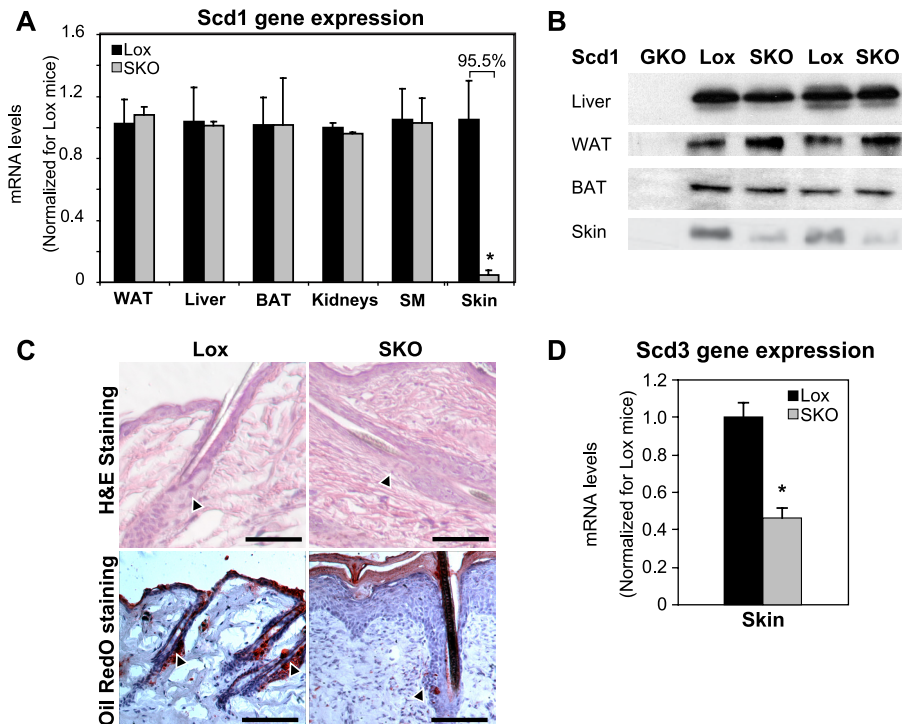
FIGURE 1. **SCD1 is deleted specifically from skin of SKO mice and causes marked sebocyte hypoplasia and reductions in sebaceous lipids.** *A,* real time PCR analysis. Analysis of *Scd1* mRNA levels in various tissues revealed that *Scd1* expression was specifically decreased only in skin of SKO mice. Results are expressed as mean ± S.E. *SM,* skeletal muscle. *B,* Western blot analysis of SCD1 protein. Protein from liver, white and brown adipose tissue, and skin revealed no changes in SCD1 levels in any tissues except skin, where it was significantly decreased in SKO mice. *C,* skin histology. Skin sections of 12-week-old male mice were stained with hematoxylin and eosin (*H&E*) (*upper panels*) or Oil Red O (*lower panels*). Both staining methods revealed a marked absence of lipid-engorged sebaceous glands (*black arrowheads*) along the hair follicles in SKO mice. Figures are representative of several animals of each genotype. *Scale bars* in all panels represent 500 μm. *D,* skin *Scd3* expression. Expression of *Scd3,* a marker of differentiated sebocytes in the skin, was measured by reverse transcription-PCR. *Scd3* expression was significantly reduced in skin of SKO mice. Results are expressed as mean ± S.E.

RESULTS

Skin-specific SCD1 Deletion Causes Sebocyte Hypoplasia—We previously generated mice with a floxed allele of *Scd1* to allow for tissue-specific deletion of the gene (16). Scd1[lox/lox] mice are phenotypically indistinguishable from wild-type mice and are used as the control mice throughout this study. The keratin-14 gene is expressed ubiquitously in the skin, including in the undifferentiated cells of the sebaceous gland (27, 28), which is the only region of skin known to express SCD1 (29). To generate skin-specific SCD1 knock-out mice (SKO), we crossed female Scd1[lox/lox] mice to male mice expressing Cre recombinase under a keratin-14 promoter (19). The resulting male Scd1[flox/+;Cre/+] mice were indistinguishable from wild-type mice in terms of appearance, viability, body weight, and food intake, indicating that the presence of Cre recombinase itself did not cause any apparent toxicity. We subsequently crossed these mice to female Scd1[lox/lox] mice to generate Scd1[lox/lox] (Lox) and Scd1[lox/lox;Cre/+] (SKO) mice. SKO mice could be easily distinguished by their closed eye fissures, dry skin, and alopecia (supplemental Fig. 1), which were apparent at weaning. Reverse transcription-PCR analysis of skin RNA from SKO mice revealed a 95% reduction in skin *Scd1* expression, relative to Lox controls (Fig. 1A), without changes in expression in liver, white (WAT) or brown adipose tissue (BAT), skeletal muscle,

or other tissues of SKO mice (Fig. 1A). SCD1 protein levels were also significantly decreased only in skin of SKO mice (Fig. 1B). A basal level of SCD1 protein was still detectable in skin of SKO mice, likely due to contamination from residual subcutaneous adipose tissue in skin samples. Given the closed eye fissure phenotype of the SKO mice, we also measured expression of *Scd1* in the Harderian gland, an eye-associated sebaceous gland (30, 31), and found that *Scd1* gene expression was decreased by over 50% in Harderian glands of SKO mice, accompanied by significant atrophy of the Harderian glands in these mice (data not shown).

To identify any structural changes in the skin, paraffin-embedded skin samples were sectioned and stained with hematoxylin and eosin. Skin sections from SKO mice revealed a marked paucity of lipid-filled sebaceous glands with foamy sebocytes that would be expected around the hair follicle (Fig. 1C). In the region where the sebaceous gland would be expected to be located (Fig. 1C, *black arrowheads*), some follicles had nodular clusters of cells, vaguely reminiscent of a sebaceous gland, but these cells never achieved the foamy vacuolation expected in mature sebocytes. Oil Red O staining of frozen skin sections confirmed the virtual absence of lipid-rich sebaceous glands in SKO mice (Fig. 1C). Consistent with the lack of mature sebocytes in the skin of SKO mice, expression of *Scd3,* a marker of differentiated sebocytes (29), was reduced by 54% in skin of SKO mice (Fig. 1D). *Scd3* is also highly expressed in the Harderian gland (32), where its expression was decreased by 50% in SKO mice (data not shown). In addition to the sebaceous gland hypoplasia, the skin of SKO mice exhibited other histologic changes previously described in a model of global SCD1 deficiency (18). For instance, the skin of SKO mice exhibited variable orthokeratotic hyperkeratosis and parakeratotic hyperkeratosis, occasional mal-aligned hair follicles, and instances of protrusion of hair shafts out of the hair follicle and into the surrounding connective tissue, with an infiltration of inflammatory cells surrounding the exposed hair shaft and keratin material (data not shown).

Skin SCD1 Deficiency Selectively Decreases Sebaceous Lipids on Skin Surface—Given the marked sebocyte hypoplasia in the skin (Fig. 1C), we hypothesized that SKO mice may have significant changes in skin lipid composition. We extracted and separated skin surface lipids by TLC. Sebaceous lipids in mice consist mainly of cholesterol esters (CE), wax mono-esters, TGs,

Skin SCD1 Deletion Increases Energy Expenditure
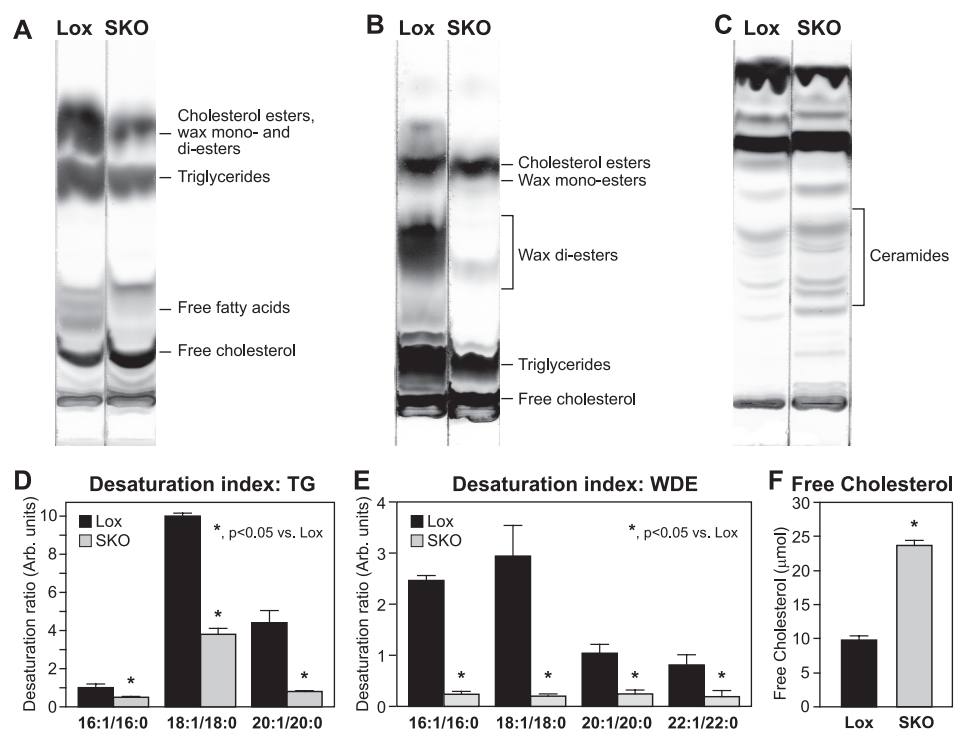
FIGURE 2. **Skin surface lipids are altered in SKO mice.** *A–C,* skin surface lipids. Skin surface lipids were extracted from Lox and SKO mice as described under "Experimental Procedures" and separated by thin layer chromatography. *D* and *E,* desaturation index. Δ-9 desaturation ratios of skin surface TGs (*D*) and WDEs (*E*) were calculated from fatty acid compositions of these lipid species analyzed by gas chromatography. *F,* levels of skin free cholesterol were measured using a colorimetric enzyme assay (Wako). *, $p < 0.05$ *versus* Lox counterparts.

TABLE 1

Fatty acid composition of skin surface lipids

Skin surface triglycerides and wax di-esters were scraped after separation by thin layer chromatography. Fatty acids were methylated and quantified by gas chromatography with penta- and heptadecanoic acids added as internal standards. Five 12-week-old male mice of each genotype were individually analyzed. Results are presented as means ± S.E. and represent total freely extractable lipids on the surface of the skin of the animal in millimoles.

Skin surface lipids	Triglycerides (mmol/animal)		Wax di-esters (mmol/animal)	
	Lox	SKO	Lox	SKO
16:0	2.58 ± 7.91	1.58 ± 0.18	0.99 ± 0.62	0.54 ± 0.02
16:1 (*n-7*)	2.33 ± 3.26	0.81 ± 0.20[a]	2.48 ± 1.63	0.13 ± 0.06[a]
18:0	1.01 ± 3.61	0.64 ± 0.05[a]	0.63 ± 0.12	0.74 ± 0.10
18:1 (*n-9*)	9.65 ± 4.56	2.20 ± 0.33[a]	1.67 ± 0.54	0.14 ± 0.00[a]
18:2 (*n-6*)	4.88 ± 2.71	1.20 ± 0.19[a]	0.38 ± 0.26	0.02 ± 0.00[a]
18:3 (*n-3*)	1.91 ± 1.01	0.07 ± 0.02[a]	0.92 ± 0.06	0.07 ± 0.02[a]
20:0	0.024 ± 0.00	0.05 ± 0.00[a]	1.21 ± 0.36	0.25 ± 0.02[a]
20:1	0.11 ± 0.05	0.04 ± 0.00[a]	0.98 ± 0.51	0.04 ± 0.03[a]
20:3 (*n-6*)	ND	ND	0.24 ± 0.11	ND[a]
20:3 (*n-9*)	ND	ND	0.29 ± 0.35	ND[a]
20:4	ND	ND	1.66 ± 0.14	0.12 ± 0.03[a]
20:5	ND	ND	0.26 ± 0.10	ND[a]
22:0	0.013 ± 0.00	0.02 ± 0.00[a]	0.53 ± 0.10	0.05 ± 0.03[a]
22:1	ND	ND	0.46 ± 0.32	0.03 ± 0.01[a]
24:00	ND	ND	0.19 ± 0.03	0.01 ± 0.00[a]
Total	25.52 ± 12.34	7.11 ± 0.89[a]	13.79 ± 3.70	2.24 ± 0.10[a]

[a] Data indicate $p < 0.05$ *versus* Lox counterparts. ND, not detectable.

was analyzed by gas chromatography (Table 1). Given the large changes in total TG and WDE levels, almost all fatty acids were significantly decreased in these fractions in SKO mice (Table 1). Notably, however, levels of palmitate (16:0) and stearate (18:0) were not significantly decreased in the WDEs (Table 1) of SKO mice. Products of Δ-9 desaturation, including 16:1, 18:1, 20:1, and 22:1, were all dramatically reduced in both TGs and WDEs (Table 1) from SKO mice, relative to Lox controls. Consequently, the Δ-9 desaturation index of skin surface lipids was significantly lowered in both the TG (Fig. 2*D*) and the WDE fractions (Fig. 2*E*) from SKO mice, relative to Lox controls, indicating that the decreased sebaceous lipids in the skin of SKO mice results from a specific loss of Δ-9 desaturase activity in the skin of these mice.

Apart from these large reductions in sebaceous lipids, we also observed a generalized increase in lipids likely to be of epidermal origin. Specifically, FC levels were increased by 2.4-fold in SKO mice (Fig. 2, *A* and *F*). In addition to FC, skin surface ceramides were also significantly increased in SKO mice, relative to Lox controls (Fig. 2*C*). Expression of hydroxymethylglutaryl-CoA reductase (*Hmgcr*; data not shown) was modestly elevated in skin of SKO mice ($p = 0.008$), suggesting increased cholesterol synthesis in the skin of these animals.

SKO Mice Have Increased Energy Expenditure and Are Resistant to High Fat Diet-induced Obesity, Adiposity, and Glucose Intolerance—To determine whether skin-specific deletion of SCD1 has any effect on energy metabolism, we measured energy expenditure in individually caged 12-week-old male Lox and SKO mice via indirect calorimetry. O_2 consumption and CO_2 production were measured for two consecutive 24-h periods with alternating 12-h dark and light cycles. SKO mice had significantly higher O_2 consumption (Fig. 3*A*) and CO_2 production (Fig. 3*B*) than Lox mice during both day and night cycles, indicating increased resting metabolic rate and increased energy expenditure in SKO mice. In fact, O_2 consumption (supplemental Fig. 2*A*) and CO_2 production (supplemental Fig. 2*B*) were increased to a similar extent in SKO mice as in mice with a global deletion of SCD1 (GKO). Similarly, heat output (kcal/h) was significantly increased in SKO mice (supplemental Fig. 2*C*) during both day and night cycles, consistent with increased energy expenditure. Respiratory quotients were similar in both Lox and SKO mice (supplemental Fig. 2*D*). Taken together, these data indicate that skin-specific deletion of SCD1 completely recapitulates the increased metabolic rate observed due to global SCD1 deletion.
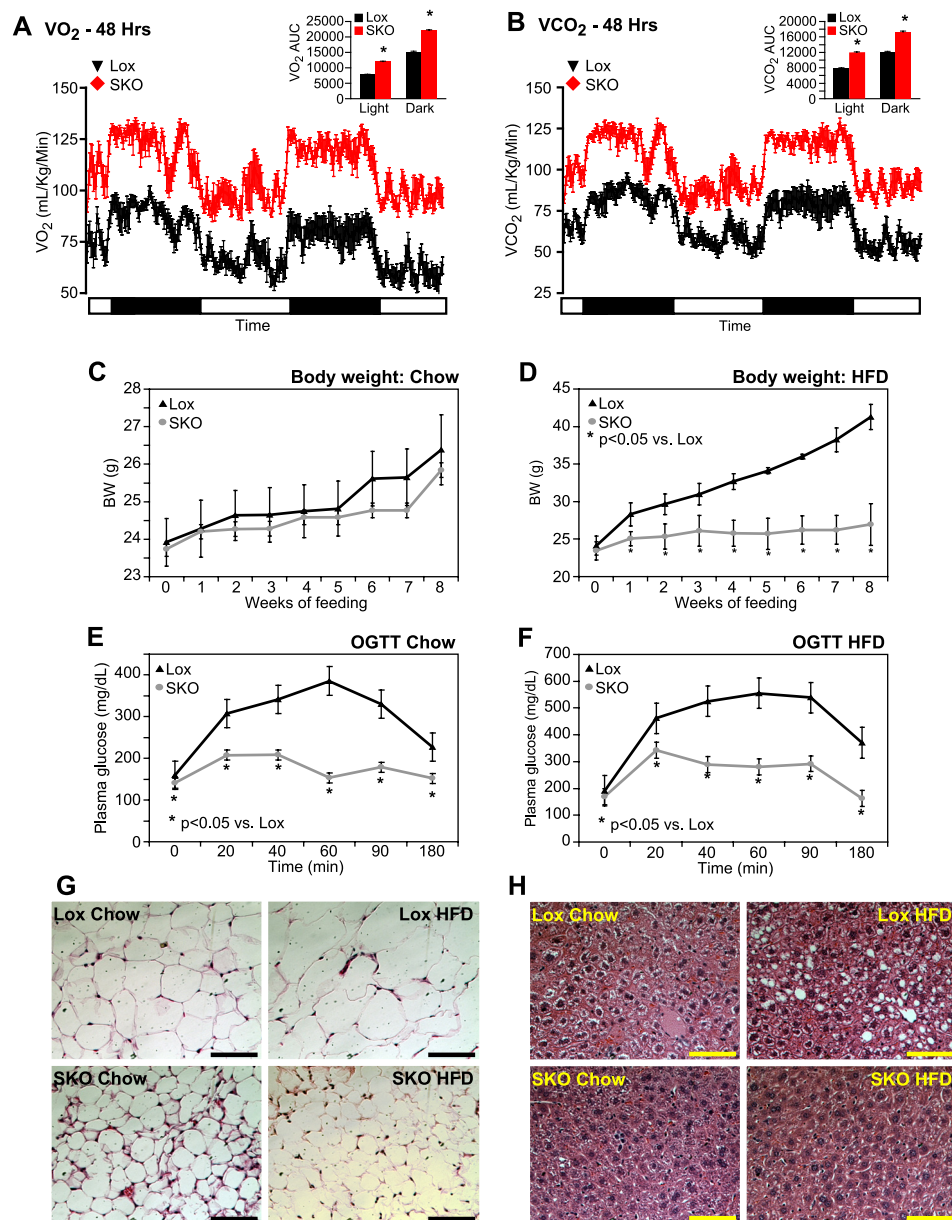
and wax di-esters (WDEs). We did not detect any significant changes in levels of either CE or wax mono-esters in skin of SKO mice (Fig. 2*B*). However, levels of the two largest lipid fractions, TGs (Fig. 2, *A* and *B*) and WDEs (Fig. 2*B*), were reduced by 72 and 84%, respectively, in skin lipids from SKO mice (Table 1). The fatty acid composition of TGs and WDEs

FIGURE 3. **SKO mice have increased energy expenditure and are protected from HFD-induced adiposity and glucose intolerance.** *A* and *B*, O_2 consumption (*A*) and CO_2 production (*B*) were measured in individually caged 12-week-old male mice in indirect calorimetry chambers. There were no significant differences in body weights of animals (Lox, 26.55 ± 0.45 and SKO, 27.05 ± 0.61 g), and data are expressed as ml/kg body weight/min of O_2 consumed (*A*) or CO_2 produced (*B*). *C* and *D*, 8-week-old male mice were fed chow (*C*) or high fat diets (*D*) for 8 weeks, and body weights were measured weekly. *E* and *F*, oral glucose tolerance (*OGTT*) was assessed after 7 weeks of feeding chow (*E*) or HFD (*F*). Mice were fasted for 4 h and administered 2 g of glucose/kg of BW by oral gavage. Data are presented as mean ± S.E. *G* and *H*, white adipose tissue (*G*) and liver (*H*) pieces were fixed in buffered formalin, and sections were stained with hematoxylin and eosin for histological examination. *Bar* represents 250 μm in all figures. *, $p < 0.05$ *versus* Lox counterparts.

weights, Lox mice gained 80% more body weight on the HFD than SKO mice (Fig. 3*D*). Glucose tolerance was assessed in SKO mice by performing oral glucose tolerance tests after 7 weeks of chow or HFD feeding. SKO mice showed significantly improved glucose tolerance curves after both chow (Fig. 3*E*) and HFD feeding (Fig. 3*F*), compared with Lox mice. Relative to Lox mice, peak plasma glucose levels were 46 and 38% lower after chow and HFD feeding, respectively, in SKO mice. Although 180-min plasma glucose levels remained elevated 1.4- and 1.9-fold over basal levels in chow- or HFD-fed Lox mice, respectively, they returned to base-line values in SKO mice, indicating improved glucose clearance in SKO mice. After HFD feeding, plasma insulin levels were significantly elevated in Lox mice, relative to chow-fed counterparts (Table 2). SKO mice, on the other hand, were protected from this diet-induced hyperinsulinemia (Table 2). Together with their improved glucose clearance (Fig. 3, *E* and *F*), these data suggest significantly improved insulin sensitivity in SKO mice.

After 8 weeks of feeding, animals were sacrificed, and epididymal WAT and subcutaneous WAT depots were weighed. Corresponding with their lower body weights, SKO mice had 53 and 76% lower epididymal WAT and 37 and 69% lower subcutaneous WAT accumulation than Lox mice on chow and HFD, respectively (Table 2). Although SKO mice did accumulate more adipose tissue after HFD feeding relative to chow-fed counterparts, they were largely resistant to the increased adiposity observed in Lox controls upon HFD feeding

Given that SKO mice have increased energy expenditure relative to Lox mice, we hypothesized that they would be protected from high fat diet (HFD)-induced obesity. 8-Week-old male Lox and SKO mice were individually caged and fed a rodent chow diet or a hypercaloric HFD (Research Diets 12492), containing 35% fat by weight (60% fat kcal). SKO mice were hyperphagic on both diets and ate 2- and 1.5-fold more than Lox mice on the chow and HFD, respectively (Table 2). Body weights were similar in both Lox and SKO animals on a chow diet (Fig. 3*C*). However, despite similar starting body

(Table 1; Fig. 3*D*). Commensurate with their decreased adiposity, both chow- and HFD-fed SKO mice had lower levels of plasma leptin relative to Lox controls (Table 2). Hematoxylin and eosin staining of epididymal WAT sections also revealed significantly smaller adipocytes in SKO mice under both chow- and HFD-fed conditions (Fig. 3*G*).

Because increased adiposity is a risk factor for hepatic lipid accumulation, livers from chow- and HFD-fed Lox and SKO mice were stained with hematoxylin and eosin. Chow-fed livers from both genotypes did not appear different from each other

TABLE 2
Food intake, body weight, serum and liver metabolites

16-Week-old male mice were sacrificed by isofluorane overdose after being fed chow or HFD for 8 weeks. Plasma glucose and insulin were measured in the same mice after 7 weeks of dietary treatment with a prior 4-h fast. All other measurements were conducted in non-fasted animals. BW, body weight; FFA, free fatty acids; T$_4$, thyroxine. Data are presented as means ± S.E.

	Lox		SKO	
	Chow	HFD	Chow	HFD
Body weight (g)	26.38 ± 0.42	41.28 ± 0.98[a]	25.84 ± 0.28	26.96 ± 1.13[b]
Food intake (g/day)	3.71 ± 0.20	2.71 ± 0.22[a]	7.45 ± 0.48[b]	4.15 ± 0.18[a,b]
Epididymal fat mass (g)	0.45 ± 0.06	3.07 ± 0.60[a]	0.21 ± 0.02[b]	0.74 ± 0.21[a,b]
Subcutaneous fat mass (g)	0.28 ± 0.03	1.49 ± 0.35[a]	0.18 ± 0.01[b]	0.47 ± 0.09[a,b]
Plasma TG (mg/dl)	62.5 ± 4.7	69.0 ± 8.0	53.6 ± 3.5	72.4 ± 5.0[a]
Plasma cholesterol (mg/dl)	110.2 ± 3.5	204.8 ± 27.9[a]	95.2 ± 4.5	119.3 ± 11.5[b]
Plasma glucose (mg/dl)	159.1 ± 14.3	191.3 ± 21.6[a]	140.4 ± 9.6	168.4 ± 11.1[a]
Plasma insulin (ng/ml)	0.77 ± 0.11	2.45 ± 0.93[a]	0.80 ± 0.36	0.83 ± 0.16[b]
Plasma leptin (ng/ml)	3.32 ± 0.67	38.49 ± 7.18[a]	0.42 ± 0.13[b]	4.36 ± 1.78[a,b]
Plasma T$_3$ (ng/dl)	87.54 ± 1.58	88.00 ± 2.40	77.09 ± 4.87	87.05 ± 13.85
Plasma T$_4$ (μg/dl)	2.80 ± 0.25	2.18 ± 0.42	1.25 ± 0.23	1.12 ± 0.25
Plasma T$_3$/T$_4$ ratio	0.03 ± 0.01	0.04 ± 0.01	0.07 ± 0.03	0.08 ± 0.01
Liver glycogen (mg/g liver)	64.59 ± 3.65	62.15 ± 3.31	29.82 ± 1.47[b]	25.71 ± 0.96[b]
Liver TG (μmol/g)	20.8 ± 5.2	98.7 ± 14.2[a]	12.7 ± 0.7[b]	33.9 ± 11.3[a,b]
Liver FFAs (μmol/g)	1.88 ± 0.18	1.79 ± 0.17	1.96 ± 0.16	1.28 ± 0.17[a,b]
Liver CE (μmol/g)	4.26 ± 0.74	10.52 ± 1.07[a]	3.19 ± 0.48[b]	8.69 ± 0.26[a,b]

[a] Data indicate $p < 0.05$ *versus* chow-fed counterparts.
[b] Data indicate $p < 0.05$ *versus* Lox counterparts.

(Fig. 3*H*). However, after HFD feeding, Lox mice had significant accumulation of hepatic lipids, which was not apparent in liver sections from SKO mice (Fig. 3*H*). Hepatic lipids were extracted and separated by TLC (supplemental Fig. 2*E*), and bands corresponding to liver free fatty acids, TGs, and CEs were scraped and quantified by gas chromatography. Although HFD feeding increased TGs and CEs in both Lox and SKO mice, SKO mice consistently had reduced hepatic TGs and CEs under both dietary conditions (Table 2). Free fatty acids levels were not different between SKO and Lox mice under chow-fed conditions (Table 2) but were decreased in SKO livers after HFD feeding, potentially due to increased esterification of fatty acids into TGs and CEs (Table 2). Analysis of fatty acid composition of these hepatic lipids revealed a generalized decrease in most major fatty acids rather than a selective decrease in any particular fatty acids (supplemental Table 1, A–C). Plasma TG was not significantly affected by genotype (Table 2). Plasma cholesterol levels increased significantly in Lox mice upon HFD feeding, but SKO mice did not show a similar increase (Table 2). Hepatic glycogen levels, a measure of the intermediate energy stores of the animal, were consistently decreased in SKO mice under both chow- and HFD-fed conditions (Table 2). Together with decreased adipose mass (Table 2), the reduced hepatic glycogen indicates reduced availability of energy reserves in SKO mice, consistent with their increased energy expenditure (Fig. 3, *A* and *B*).

Hepatic Induction of Genes of de Novo Lipogenesis Is Not Impaired in SKO Mice—To determine whether the lower hepatic lipid accumulation and protection from diet-induced obesity are a consequence of decreases in the *de novo* lipogenesis pathway, we measured hepatic expression of key lipogenic genes (Fig. 4*A*). On a chow diet, SKO mice had significantly lower expression of lipogenic genes, including acetyl-CoA carboxylase (*Acc*), fatty-acid synthase (*Fas*), and *Scd1* (Fig. 4*A*). Also, expression of the lipogenic transcription factor, sterol-regulatory element binding protein-1c (*Srebp-1c*), and its requisite co-activator, PPAR-γ co-activator-1β (*Pgc-1β*), were significantly lower in SKO mice, relative to Lox counterparts.

After HFD feeding, levels of all lipogenic genes, except *Srebp-1c*, were normalized in SKO mice, relative to Lox controls (Fig. 4*A*). Although the magnitude of change from chow to HFD was similar in both SKO and Lox mice, *Srebp-1c* gene expression remained significantly lower in SKO mice (Fig. 4*A*), suggesting either that this level of induction of *Srebp-1c* and *Pgc-1β* is sufficient to restore lipogenic gene expression or that an alternative *Srebp-1c*-independent mode of regulation normalizes lipogenic genes in HFD-fed SKO mice.

SREBP-1c is also regulated post-translationally by proteolytic processing of the precursor protein and transit of the mature form to the nucleus (33). Under chow-fed conditions, SKO mice had significantly lower nuclear levels of the mature SREBP-1 protein (Fig. 4*B*), corresponding to the decreased expression of hepatic lipogenic genes (Fig. 4*A*). After HFD feeding, nuclear levels of SREBP-1 were still lower in SKO mice, relative to Lox controls, but the difference in nuclear SREBP-1 protein levels between Lox and SKO mice was attenuated. This was consistent with the rescue of lipogenic gene expression in HFD-fed SKO mice (Fig. 4*A*), suggesting that impaired lipogenesis is not likely to be the cause of decreased hepatic lipid accumulation in these mice. In contrast, GKO mice had lower nuclear SREBP-1 protein (supplemental Fig. 3*A*) and reduced hepatic lipogenic gene expression (supplemental Fig. 3*B*) relative to control mice on a chow diet, which was not rescued even after HFD feeding.

To confirm further that SKO mice are able to induce *de novo* lipogenic genes in response to a dietary stimulus, we subjected Lox and SKO mice to a fasting-refeeding protocol known to robustly induce *de novo* lipogenesis in the liver. Consistent with their increased energy expenditure, SKO mice lost more body weight in response to fasting than Lox controls (2.7 ± 0.5 g *versus* 1.4 ± 0.5 g; $p = 0.0002$). However, upon being given access to food (high carbohydrate diet), SKO mice consumed significantly more food than Lox counterparts (3.02 ± 0.56 g *versus* 2.07 ± 0.24 g; $p = 0.0009$), and regained all body weight lost. Thus, this acute fasting-refeeding protocol did not cause any net changes in body weight in either Lox or SKO mice. As

A

Hepatic lipogenic genes

B

C

D

**Hepatic lipogenic genes
Fasting-refeeding**
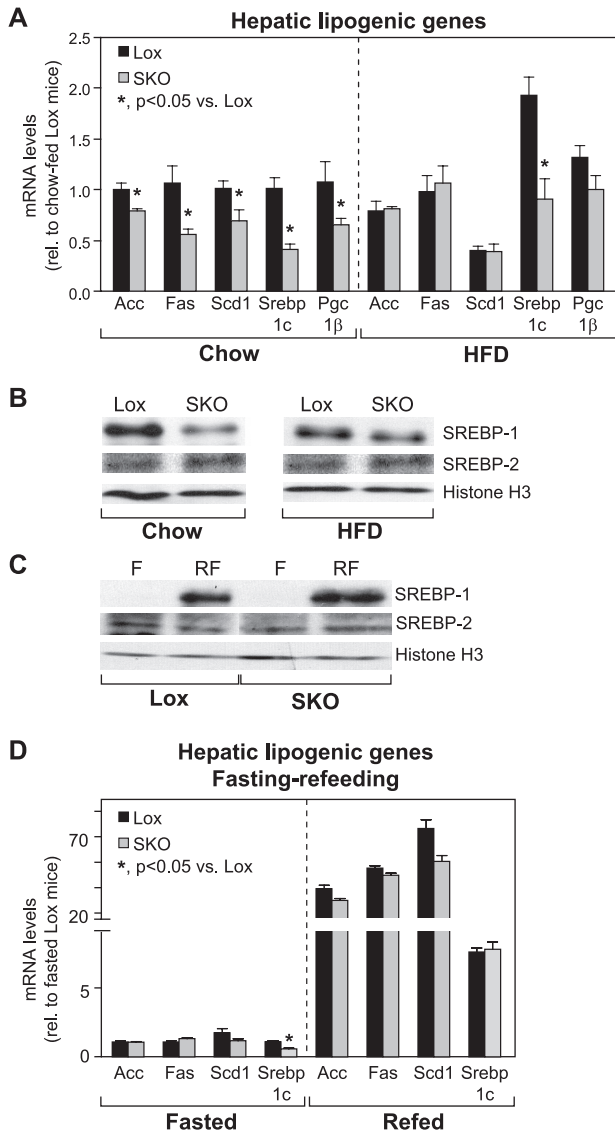
FIGURE 4. **Hepatic lipogenic gene expression is not decreased in HFD-fed or fasted-refed SKO mice.** *A* and *B,* hepatic lipogenic gene expression (*A*) and nuclear levels of SREBP-1, SREBP-2, and histone H$_3$ (*B*) were measured in Lox and SKO mice after 8 weeks of chow or HFD feeding. *, $p < 0.05$ *versus* Lox counterparts. *C* and *D,* induction of nuclear levels of SREBP-1 (*C*) and lipogenic genes (*D*) was measured in livers of mice fasted for 12 h or fasted and refed a high carbohydrate lipogenic diet for 12 h. Data are presented as means ± S.E. *, $p < 0.05$ *versus* Lox counterparts. *Acc,* acetyl-CoA carboxylase; *F,* fasted; *Fas,* fatty-acid synthase; *Pgc-1β,* PPAR-γ co-activator-1β; *RF,* fasted-refed; *Scd1,* stearoyl-CoA desaturase-1; *Srebp-1c,* sterol regulatory element-binding protein-1c.

anticipated, Lox mice responded to refeeding a lipogenic diet by dramatically increasing both nuclear levels of mature SREBP-1 (Fig. 4*C*) as well as hepatic lipogenic genes, including *Acc, Fas, Scd1, Srebp-1c,* and *Pgc-1β* (Fig. 4*D*). Similarly, SKO mice also responded to refeeding with a robust increase in SREBP-1 maturation (Fig. 4*C*) and hepatic expression of key lipogenic genes, to the same extent as Lox mice (Fig. 4*D*). In contrast, GKO mice subjected to the same fasting-refeeding challenge had significantly lower levels of both nuclear SREBP-1 (supplemental Fig. 3*C*) as well as hepatic lipogenic gene expression (supplemental Fig. 3*D*). These results clearly demonstrate that unlike global SCD1 deletion, skin-specific deletion of SCD1 does not impair

the hepatic *de novo* lipogenic pathway and that impaired lipogenesis is not likely to be the basis of protection from diet-induced obesity in SKO mice. Thus, the reduction of hepatic lipogenesis because of global SCD1 deletion (supplemental Fig. 3) is likely to be mediated by SCD1 in the liver (16).

Expression of Genes of Fatty Acid Oxidation, Lipolysis, and Uncoupling Is Induced in SKO Mice—Given that hepatic lipogenesis was unaffected in SKO mice after HFD feeding, we hypothesized that net increases in catabolic processes in the liver and other peripheral tissues may underlie the protection from diet-induced obesity and adiposity observed in SKO mice. We therefore measured markers of fatty acid oxidation, lipolysis, and thermogenesis in peripheral tissues, including liver, skeletal muscle, and brown and white adipose tissues of chow- or HFD-fed SKO mice. Expression of the key genes of fatty acid oxidation, carnitine palmitoyltransferase-1 (*Cpt-1*) and acyl-CoA oxidase (*Aox*), was modestly elevated in livers of SKO mice, relative to Lox counterparts, under both dietary conditions (Fig. 5*A*). Expression of the transcriptional co-activator *Pgc-1α,* which mediates aspects of the fasted response in liver, was increased by 1.5-fold in livers of chow-fed SKO mice; after HFD feeding, *Pgc-1α* levels were increased in Lox controls and hence were not significantly different between Lox and SKO mice (Fig. 5*A*). Expression of *Ucp-2* and *-5* was significantly induced in SKO mice after both chow as well as HFD feeding. Although the exact contribution of hepatic uncoupling to energy expenditure is still under debate, it is possible that the increased levels of *Ucps* in liver contribute to increased proton dissipation, thereby increasing resting metabolic rate and energy expenditure (34).

In rodents and humans, skeletal muscle is a major site of energy metabolism and contributes significantly to whole body thermogenesis. Even slight increases in levels of UCP-2 and UCP-3 in skeletal muscle have been shown to be protective against obesity (35–40). We observed a 1.7–2-fold increase in expression of both *Ucp-2* and *Ucp-3* in skeletal muscle of SKO mice (Fig. 5*B*), which could contribute to their observed protection from diet-induced obesity. PPAR-γ co-activator-1α (*Pgc-1α*), a known co-activator of genes encoding for uncoupling proteins (41), was also induced in muscle of SKO mice (Fig. 5*B*). In addition to these thermogenic genes, expression of lipoprotein lipase (*Lpl*) was modestly induced in muscle of SKO mice (Fig. 5*B*), suggesting increased lipid uptake in skeletal muscle. Increased lipid uptake through lipoprotein lipase in skeletal muscle has been suggested to channel lipids toward oxidation rather than storage (42). Increased WAT uncoupling via UCP-1 has been shown to confer protection against diet-induced obesity by increasing the thermogenic capacity of WAT (43–45). In WAT of chow-fed SKO mice, we detected a 2.5-fold ($p = 0.05$) increase in *Ucp-1* expression, relative to Lox controls (Fig. 5*C*). After HFD feeding, *Ucp-1* levels tended to remain higher in SKO mice by up to 4-fold on average (Fig. 5*C*); however, inter-animal variability kept this difference from being statistically significant. We also detected a 1.9–2.8-fold increase in levels of *Pgc-1α,* an important co-activator of *Ucp-1* (46, 47), in WAT of chow- and HFD-fed SKO mice, respectively (Fig. 5*C*). Expression of *Ucp-3,* which is also generally restricted to BAT and muscle in rodents (48, 49), was modestly increased
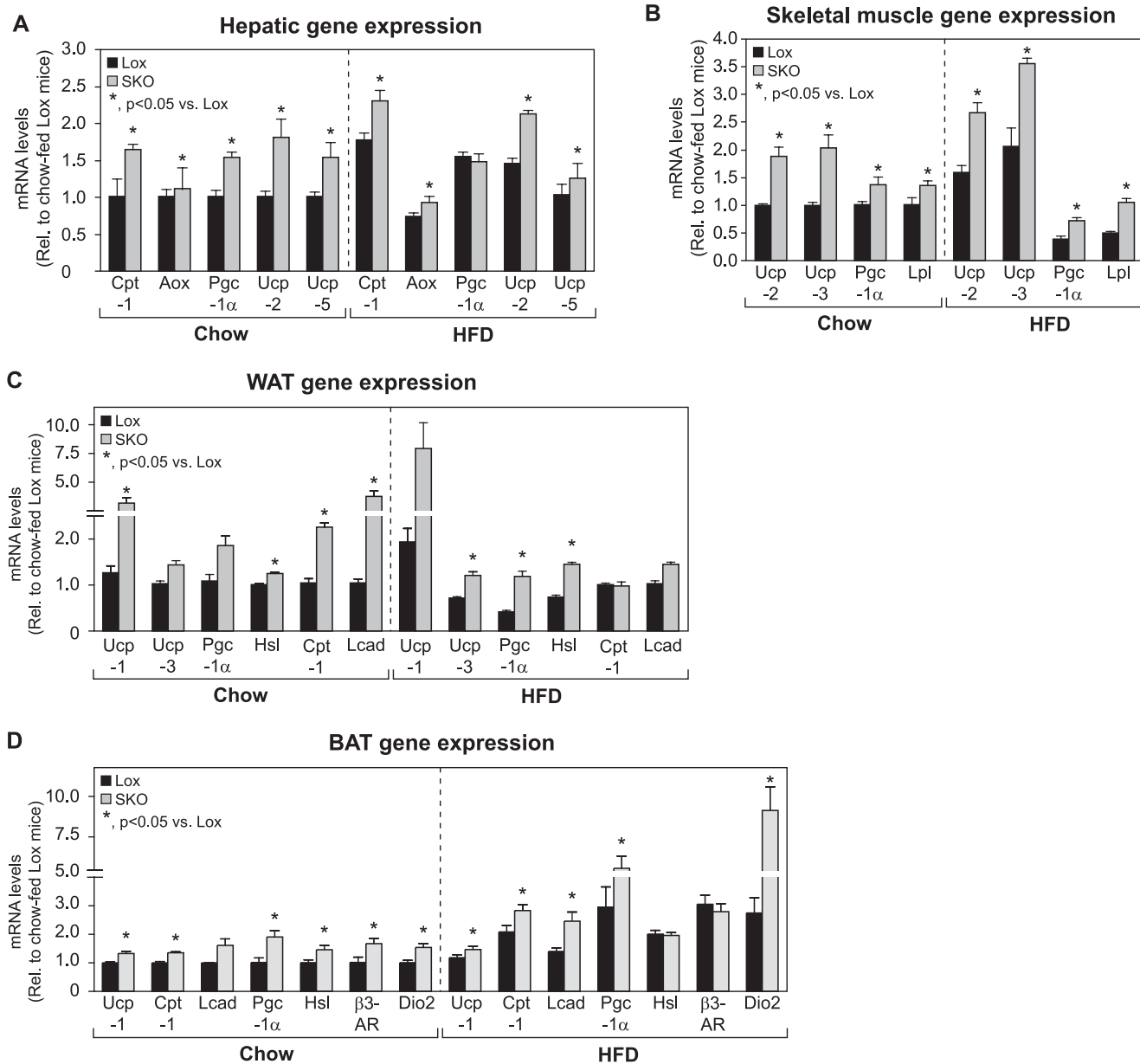
FIGURE 5. **Expression of oxidative, lipolytic, and thermogenic genes is altered in peripheral tissues of SKO mice.** *A–D,* expression of genes involved in uncoupling, lipid uptake, lipolysis, and fatty acid oxidation was measured in liver (*A*), skeletal muscle (*B*), WAT (*C*), and BAT (*D*) of chow- or HFD-fed SKO and Lox mice. Data are presented as means ± S.E. *, *p* < 0.05 *versus* Lox counterparts. *Aox,* acyl-CoA oxidase; *β3-AR,* β_3-adrenergic receptor; *Cpt-1,* carnitine palmitoyl-transferase-1; *Dio2,* type II iodothyronine deiodinase; *Hsl,* hormone-sensitive lipase; *Lcad,* long-chain acyl-CoA dehydrogenase; *Lpl,* lipoprotein lipase; *Pgc-1α,* PPAR-γ co activator-1α; *Ucp,* uncoupling protein.

by 1.4-fold ($p = 0.06$) and 1.7-fold ($p = 0.007$) in WAT of chow- and HFD-fed SKO mice, respectively (Fig. 5*C*). *Ucp-2* expression was not increased in WAT of SKO mice (data not shown). Under chow-fed conditions, oxidative genes, including *Cpt-1* and long-chain acyl-CoA dehydrogenase (*Lcad*), were increased by 2.3- and 3.4-fold, respectively, in SKO mice (Fig. 5*C*); this difference was not observed in HFD-fed animals (Fig. 5*C*). Hormone-sensitive lipase (*Hsl*) expression was modestly increased by 1.3–1.6-fold in chow- and HFD-fed SKO mice, respectively (Fig. 5*C*), suggesting a more catabolic state in WAT of SKO mice, consistent with their decreased adipose mass (Table 2). We did not observe any significant differences in levels of *Ppar-γ*, *Fas*, or *Scd1* in WAT of SKO animals (data not shown), suggesting that there was no defect in adipocyte differ-

entiation that could account for decreased adipose mass in SKO mice.

BAT is a major site of thermogenesis in rodents and expresses high levels of UCP-1. UCP-1 is induced by cold exposure and contributes to heat generation at the expense of ATP production, thereby increasing energy expenditure in the whole animal (46, 50, 51). *Ucp-1* expression was modestly elevated in BAT of both chow- and HFD-fed SKO mice, relative to Lox counterparts (Fig. 5*D*). Furthermore, expression of BAT *Pgc-1α*, which is known to be robustly induced in response to cold exposure (51), was increased by 2- and 2.5-fold in chow- and HFD-fed SKO mice, respectively (Fig. 5*D*). Expression of genes of fatty acid oxidation, including *Cpt-1* and *Lcad,* was induced by 1.2- and 1.6-fold, respectively, in SKO mice under
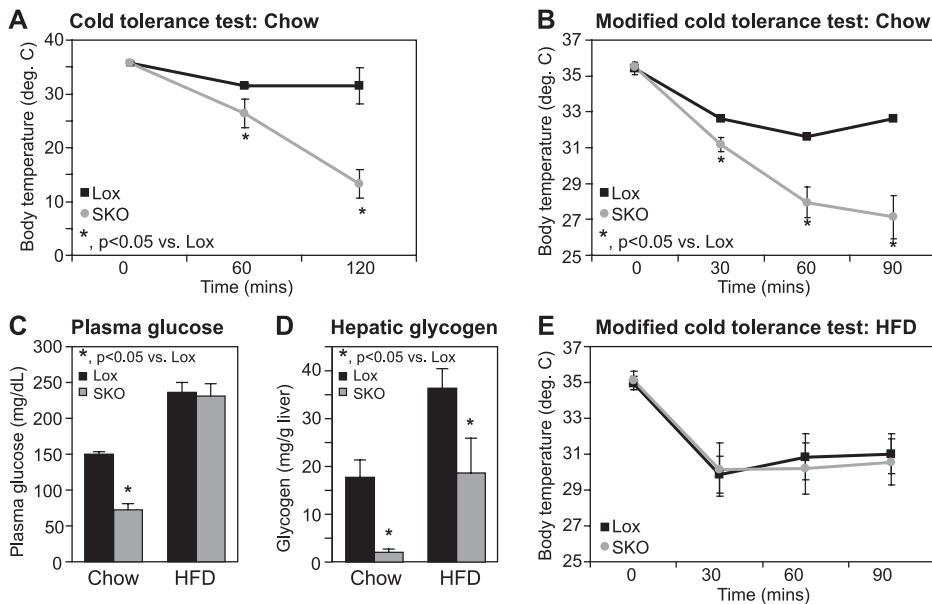
FIGURE 6. **Cold tolerance is impaired in SKO mice because of rapid depletion of hepatic glycogen.** *A* and *B*, 12-week-old chow-fed Lox and SKO mice were exposed to 4 °C for 120 min (*A*) or for a shorter duration of 90 min (*B*) with *ad libitum* access to chow diet and water. Rectal temperatures were measured at the indicated time points with a YSI Inc. series precision thermometer. *C*, blood was collected by cardiac puncture following euthanasia, and blood glucose was measured by the glucose oxidase method. *D*, hepatic glycogen was measured by an enzyme-coupled spectrophotometric assay. *E*, 9-week-old Lox and SKO mice were fed a high fat diet for 3 weeks and subjected to a cold tolerance test. Detailed diet composition is available in the supplemental Methods. *, $p < 0.05$ *versus* Lox counterparts.

peratures were not different between Lox and SKO mice (Fig. 6*A*). However, upon cold exposure, SKO animals displayed a severe inability to maintain body temperature (Fig. 6*A*), and all SKO mice went into a state of extreme lethargy progressing to death within 3 h. For subsequent experiments, we adopted a modified cold exposure protocol of subjecting all animals to 4 °C for 90 min, to be able to study animals prior to the onset of torpor. Despite starting at similar body temperatures, within 90 min of cold exposure, SKO mice displayed an 8.4 °C drop in body temperature, whereas Lox mice only had a 2.4 °C change (Fig. 6*B*). Although basal plasma glucose levels were similar in SKO and Lox mice maintained on a chow diet (Table 2), SKO mice had a significant reduction in plasma glucose levels within 90 min of cold exposure (Fig. 6*C*), suggesting hypoglycemia to be a potential cause of death in cold-exposed SKO mice.

Hepatic glycogen levels were ~50% lower in chow-fed SKO mice under basal conditions (Table 2), indicating decreased energy reserves in these mice, consistent with their increased energy expenditure. After cold exposure for 90 min, both Lox and SKO mice had reduced hepatic glycogen stores (Fig. 6*D*), as expected, because hepatic glycogen is an important energy source during cold exposure (20, 58). However, consistent with their hypoglycemia (Fig. 6*C*), cold-exposed SKO mice had a near complete depletion of hepatic glycogen to about 11% of the values seen in Lox controls (Fig. 6*D*).

Given the increased energy expenditure observed in SKO mice coupled with alopecia and loss of skin sebaceous lipids, we hypothesized that SKO mice may lose more heat through their skin and therefore utilize more substrates for heat production. If this were the case, we hypothesized that prior feeding of SKO mice with a hypercaloric diet may help bolster their fuel reserves and attenuate the cold intolerance observed in these mice. We therefore placed SKO mice on a 20% by weight high fat diet for 3 weeks. We formulated the diets with either saturated fat from fully hydrogenated coconut oil or monounsaturated fat (MUFA) from high oleic safflower oil as the predominant fat source. Because both diets elicited the same response in Lox and SKO mice, only the data from the MUFA feeding are shown. Over the 3 weeks of HFD feeding, SKO mice gained 0.82 ± 0.69 g, whereas Lox mice gained 5.85 ± 0.70 g of body weight. After HFD feeding for 3 weeks, Lox and SKO mice were subjected to another cold tolerance test. HFD-fed SKO were now able to regulate their body temperatures similar to Lox counterparts (Fig. 6*E*) and were able to tolerate prolonged cold exposure, similar to Lox controls (over 24 h; data not shown). Unlike chow-fed SKO mice (Fig. 6*C*), HFD-fed SKO mice were

both dietary conditions (Fig. 5*D*). Furthermore, expression of *Hsl* and β_3-adrenergic receptor ($\beta3$-*Ar*) expression was elevated in chow-fed SKO mice (Fig. 5*D*). Taken together, these results indicate a catabolic state of increased lipolysis and lipid oxidation in BAT of SKO mice, along with increased uncoupling via *Ucp-1* and *Pgc-1α*.

Thyroid hormone signaling is also an activator of BAT thermogenesis (52, 53), and in addition to being derived from the circulation, T_3 can be generated *in situ*, by type II iodothyronine deiodinase (DIO2), which is chiefly expressed in BAT of rodents (53, 54). Increased BAT *Dio2* expression has been shown to increase energy expenditure, potentially through increased uncoupling via *Ucp-1* and *Pgc-1α*, and confer resistance to diet-induced obesity in mice (55–57). Although activation of plasma membrane receptors such as β_3-adrenergic receptor and consequent generation of cAMP has been shown to activate *Dio2* expression, the *Dio2* gene can also be regulated independently of cAMP, especially under conditions such as HFD feeding (56, 57). We found that in BAT of chow-fed SKO mice, *Dio2* expression was modestly increased by 1.5-fold, relative to Lox counterparts (Fig. 5*D*). However, upon HFD feeding, SKO mice had 3.3-fold higher *Dio2* expression than Lox counterparts (Fig. 5*D*), corresponding with their protection from HFD-induced obesity.

SKO Mice Have Severe Cold Sensitivity Because of Rapid Hepatic Glycogen Depletion and Hypoglycemia—Environmental temperatures are a strong determinant of adaptive thermogenesis in homeotherms. Therefore, to test if response to cold exposure is altered in the hypermetabolic SKO mice, we subjected Lox and SKO animals to a 4 °C cold challenge and monitored changes in core body temperature. Starting body tem-

able to maintain plasma glucose at steady state levels even after cold exposure (Fig. 6*C*). Although chow-fed SKO mice showed a drastic depletion of hepatic glycogen upon cold exposure (Fig. 6*D*), prior high fat feeding in SKO mice did not result in a similar ablation of hepatic glycogen during cold exposure (Fig. 6*D*). This sparing of hepatic glycogen corresponded well with the prevention of hypoglycemia (Fig. 6*C*) and improved cold tolerance (Fig. 6*E*) observed in SKO mice fed a HFD prior to cold exposure.

DISCUSSION

Apart from acting as the first line of defense, the skin is also a site of active lipid synthesis. The lipid profile of the skin affects one of its most important functions of serving as a barrier against heat and water loss to the environment (59, 60). Mice with a global SCD1 deficiency have severe impairments in the structure of the skin, characterized by sebaceous gland hypoplasia, dry skin, and alopecia (17, 18, 61–63). SCD1-deficient mice also have a hypermetabolic phenotype and have been shown to be resistant to weight gain, despite persistent hyperphagia (4, 6–8). However, the contributions of SCD1 in various peripheral tissues to this global metabolic phenotype were as yet unclear. The results of our present study indicate that the cutaneous phenotypes resulting from global SCD1 deletion are a direct result of the loss of SCD1 and local Δ-9 MUFA synthesis in the skin. Furthermore, these data suggest that these cutaneous alterations are intricately linked to changes in systemic energy metabolism. To the best of our knowledge, these mice represent the first model of skin-specific deletion of a lipogenic enzyme resulting in global changes in energy homeostasis.

The reduction of sebaceous lipids upon deletion of skin SCD1 (Fig. 2*B*) may be of value in the treatment of human diseases such as acne vulgaris, which are associated with increased sebaceous activity. Although the mechanisms for sebocyte hypoplasia because of SCD1 deficiency have yet to be determined, it is tempting to speculate that the concurrent accumulation of FC in the skin of SKO mice (Fig. 2, *A* and *F*) plays a role in this process. Indeed, other mouse models, including mice overexpressing human apolipoprotein C1 (64), a constituent of very low density lipoproteins, and mice deficient in acyl-CoA:cholesterol acyltransferase-1 (65), the major enzyme of cholesterol esterification, all have increased levels of skin FC and similar cutaneous phenotypes as SKO mice (64, 65). Alternatively, skin SCD1 deficiency could result in altered levels of important metabolites that regulate sebocyte differentiation and proliferation. For instance, loss of SCD1 activity in the skin may result in decreased synthesis of ligands for activation of PPAR isoforms in the skin that are thought to be required for sebocyte development (66, 67). Alternatively, decreased retinol esterification in the skin has been recently suggested as a potential cause for sebocyte atrophy (68). Because one of the storage forms of retinol is as retinyl oleate, decreased skin oleate pools in SKO mice (Table 1) may result in decreased retinol esterification, thereby contributing to the sebocyte hypoplasia in SKO mice (Fig. 1*C*). Given the heterogeneity of cells in the skin, future studies specifically focused on sebaceous cells are neces-

sary to resolve the mechanistic contribution of SCD1 to sebocyte differentiation and proliferation.

It has been suggested that global loss of SCD1 may cause an alteration in skin barrier permeability and increase water loss through the skin (18, 63). Although we did not measure transepidermal water loss in this study, our findings of increased skin FC and ceramides (Fig. 2) were in contrast to reported decreases in skin sterols (18) and ceramides (63) in mice with global SCD1 deficiency, suggesting important differences between these mouse models and our current model of skin SCD1 deletion. Similar to the SKO mice, a separate mouse model of global SCD1 deficiency (asebia J1 mice) has been shown to have intact barrier function despite sebocyte atrophy (61), suggesting that loss of sebaceous lipids *per se* does not alter barrier function in mice (18, 61). As observed in SKO mice (Fig. 2, *A* and *C*), asebia J1 mice also do not have decreased epidermal lipids, including ceramides and cholesterol (61). Because increases in skin surface FC and ceramides have been reported to be essential for recovery following acute skin barrier disruption (59, 60, 69), the increase in these lipids in skin of SKO mice (Fig. 2) may represent a compensatory mechanism to preserve barrier homeostasis in the context of sebocyte hypoplasia.

At 25 °C, room temperature is 5–7 °C below thermoneutrality in a mouse (70), and metabolic efficiency is compromised under these conditions to maintain core body temperature (71, 72). Organisms have developed a variety of ways to sacrifice fuel efficiency to maintain temperature homeostasis, one of which is the uncoupling of respiration from ADP phosphorylation via mitochondrial UCPs (73). UCP-1 in BAT of rodents is robustly induced in response to cold, and it has been established as an important regulator of temperature and energy homeostasis (50, 51, 71, 74). Additionally, uncoupling in other tissues such as skeletal muscle via UCP-2 and -3 also contributes to the thermogenic response to cold exposure (50, 51, 74). The induction of BAT *Ucp-1* (Fig. 5*D*) along with *Pgc-1α* in BAT and skeletal muscle (Fig. 5, *D* and *B*) of SKO mice maintained at room temperature suggests increased need for heat generation in SKO mice, as both *Ucp-1* and *Pgc-1α* are known to be strongly induced by cold exposure (50, 51, 75).

The importance of ambient temperature to the development of obesity in rodents has been elegantly demonstrated in mice lacking UCP-1. $UCP-1^{-/-}$ mice are resistant to diet-induced obesity at temperatures below 20 °C but prone to obesity when maintained at thermoneutrality (58, 71, 76). Because SKO mice lack insulating factors, including fur and sebaceous lipids, it is likely that cold perception is heightened in these animals, thereby necessitating an increase in basal thermogenesis for temperature maintenance, at the expense of fuel economy. This increased thermogenic demand in SKO mice is met partially through increased food consumption (Table 2) as well as increased lipid and glucose oxidation, as evidenced by higher O_2 consumption (Fig. 3*A*) and decreased fat and glycogen storage (Table 2). Additionally, SKO mice are acutely cold-intolerant, rapidly depleting energy substrates upon cold exposure (Fig. 6). These observations lend further support to the hypothesis that increased cold perception in SKO mice underlies their protection from diet-induced obesity. Interestingly, similar phenotypes of resistance to diet-induced obesity have been

described in other mouse models that exhibit cutaneous changes, including mice globally deficient in DGAT1 (68, 77, 78), mice overexpressing human apolipoprotein C1 (64, 79), and mice lacking the vitamin D receptor (44, 80). Although a link between the skin phenotypes and energy expenditure has not been inferred in these mouse models, the data from this study suggest that, in addition to ambient temperatures, cutaneous changes are an important consideration in metabolic studies utilizing transgenic mice.

Induction of UCP-1 in WAT has been shown to be protective against diet-induced obesity in multiple mouse models, including liver X receptor knock-out mice and mice lacking the vitamin D receptor (43, 44, 50, 75). In SKO mice, the increases in WAT *Ucp-1* levels were relatively subtle, as compared with other obesity-resistant models that have reported as much as a 25-fold increase in WAT *Ucp-1* expression (44). Although some SKO mice in this study did indeed exhibit changes as large as 30-fold or even higher in WAT *Ucp-1* expression, most animals had a more modest elevation of WAT *Ucp-1*. Also, whereas adipocytes from WAT of SKO mice were significantly smaller (Fig. 3*G*), we did not observe a perceptible change in the color of fat pads or a significant increase in cells with multiple lipid droplets, as is characteristic of brown adipocytes. Nonetheless, the modest but consistent increases in *Ucp-1* in WAT of SKO mice (Fig. 5*C*), in conjunction with the increased expression of *Ucps* in BAT (Fig. 5*D*) and skeletal muscle (Fig. 5*B*), could plausibly contribute to significantly increased uncoupling in peripheral tissues of these animals. Such an elevation in uncoupling would be expected to place a tremendous demand on the energy reserves of the animal, thereby dissipating excess calories as heat and conferring protection from diet-induced obesity, as observed in SKO mice.

Uncoupling in liver, skeletal muscle, and adipose tissue can be activated through PPARα activation, increased thyroid hormone signaling, increased free fatty acid levels, or increased β-adrenergic signaling (50, 75, 81). Increased fatty acid uptake through *Lpl* in skeletal muscle (Fig. 5*B*) or increased lipolysis through *Hsl* in WAT (Fig. 5*C*) could both transiently increase the local levels of free fatty acids, thereby contributing to induction of *Ucps* in SKO mice. Alternatively, it is possible that increased signaling through either the β_3-adrenergic receptor or through serum or tissue T_3 is responsible for increased uncoupling in SKO mice. Consistent with this hypothesis, expression of BAT *Dio2* was significantly elevated in SKO mice, especially upon HFD feeding (Fig. 5*D*). *Dio2* expression in BAT leads to local increases in T_3 signaling without changes in circulating T_3 levels, and increased BAT *Dio2* is strongly associated with increased energy expenditure and obesity resistance in mice (52–56, 58). Taken together with the increased markers of lipid oxidation and uncoupling in BAT (Fig. 5*D*), the large increase in *Dio2* gene levels (Fig. 5*D*) could contribute to the protection from diet-induced obesity observed in SKO mice.

In summary, the results of this study elucidate a role for skin SCD1 and local synthesis of Δ-9 MUFAs not only in maintaining the structure and lipid composition of the skin but also in altering global energy balance. Unlike GKO mice (supplemental Fig. 3) and mice with liver-specific ablation of

SCD1 (16), hepatic lipogenesis is not severely impaired in SKO animals (Fig. 4), further confirming our previous finding that *de novo* lipogenesis is mainly regulated by hepatic SCD1 (16). Although studies targeting hepatic and adipose SCD1 using antisense-mediated approaches have described protection from diet-induced obesity and insulin resistance (11–13), we have previously reported that chronic deletion of hepatic SCD1 does not protect mice against the detrimental effects of high fat diets (16). In fact, the results of this study suggest that a major part of the hypermetabolic phenotype of global SCD1 deletion in mice is mediated by loss of SCD1 in the skin and not the liver. These data do not necessarily exclude a role for SCD1 in other tissues such as brown or white adipose tissue, because the severity of the cutaneous phenotypes in SKO mice may mask the contributions of SCD1 in these tissues to global energy homeostasis. Nevertheless, these data reveal an as yet underappreciated role for local synthesis of MUFAs in the skin to maintaining skin lipid composition and illustrate an example of cross-talk between the skin and peripheral organs in the regulation of whole body energy metabolism.

REFERENCES

1. Mensah, G. A., Mokdad, A. H., Ford, E., Narayan, K. M., Giles, W. H., Vinicor, F., and Deedwania, P. C. (2004) *Cardiol. Clin.* **22,** 485–504
2. Grundy, S. M. (2007) *J. Clin. Endocrinol. Metab.* **92,** 399–404
3. Muoio, D. M., and Newgard, C. B. (2006) *Annu. Rev. Biochem.* **75,** 367–401
4. Miyazaki, M., Dobrzyn, A., Man, W. C., Chu, K., Sampath, H., Kim, H. J., and Ntambi, J. M. (2004) *J. Biol. Chem.* **279,** 25164–25171
5. Miyazaki, M., Kim, Y. C., Gray-Keller, M. P., Attie, A. D., and Ntambi, J. M. (2000) *J. Biol. Chem.* **275,** 30132–30138
6. Miyazaki, M., Kim, Y. C., and Ntambi, J. M. (2001) *J. Lipid Res.* **42,** 1018–1024
7. Ntambi, J. M., Miyazaki, M., Stoehr, J. P., Lan, H., Kendziorski, C. M., Yandell, B. S., Song, Y., Cohen, P., Friedman, J. M., and Attie, A. D. (2002) *Proc. Natl. Acad. Sci. U.S.A.* **99,** 11482–11486
8. Cohen, P., Miyazaki, M., Socci, N. D., Hagge-Greenberg, A., Liedtke, W., Soukas, A. A., Sharma, R., Hudgins, L. C., Ntambi, J. M., and Friedman, J. M. (2002) *Science* **297,** 240–243
9. Rahman, S. M., Dobrzyn, A., Dobrzyn, P., Lee, S. H., Miyazaki, M., and Ntambi, J. M. (2003) *Proc. Natl. Acad. Sci. U.S.A.* **100,** 11110–11115
10. Rahman, S. M., Dobrzyn, A., Lee, S. H., Dobrzyn, P., Miyazaki, M., and Ntambi, J. M. (2005) *Am. J. Physiol. Endocrinol. Metab.* **288,** E381–387
11. Jiang, G., Li, Z., Liu, F., Ellsworth, K., Dallas-Yang, Q., Wu, M., Ronan, J., Esau, C., Murphy, C., Szalkowski, D., Bergeron, R., Doebber, T., and Zhang, B. B. (2005) *J. Clin. Invest.* **115,** 1030–1038
12. Gutiérrez-Juárez, R., Pocai, A., Mulas, C., Ono, H., Bhanot, S., Monia, B. P., and Rossetti, L. (2006) *J. Clin. Invest.* **116,** 1686–1695
13. Brown, J. M., Chung, S., Sawyer, J. K., Degirolamo, C., Alger, H. M., Nguyen, T., Zhu, X., Duong, M. N., Wibley, A. L., Shah, R., Davis, M. A., Kelley, K., Wilson, M. D., Kent, C., Parks, J. S., and Rudel, L. L. (2008) *Circulation* **118,** 1467–1475
14. Choi, C. S., Savage, D. B., Kulkarni, A., Yu, X. X., Liu, Z. X., Morino, K., Kim, S., Distefano, A., Samuel, V. T., Neschen, S., Zhang, D., Wang, A., Zhang, X. M., Kahn, M., Cline, G. W., Pandey, S. K., Geisler, J. G.,

Bhanot, S., Monia, B. P., and Shulman, G. I. (2007) *J. Biol. Chem.* **282,** 22678–22688

15. Levin, A. A., Yu, R. Z., and Geary, R. S. (2008) in *Antisense Drug Technology* (Crooke, S. T., ed.) 2nd Ed., pp. 183–216, CRC Press, Inc., Boca Raton, FL

16. Miyazaki, M., Flowers, M. T., Sampath, H., Chu, K., Otzelberger, C., Liu, X., and Ntambi, J. M. (2007) *Cell Metab.* **6,** 484–496

17. Miyazaki, M., Man, W. C., and Ntambi, J. M. (2001) *J. Nutr.* **131,** 2260–2268

18. Sundberg, J. P., Boggess, D., Sundberg, B. A., Eilertsen, K., Parimoo, S., Filippi, M., and Stenn, K. (2000) *Am. J. Pathol.* **156,** 2067–2075

19. Dassule, H. R., Lewis, P., Bei, M., Maas, R., and McMahon, A. P. (2000) *Development* **127,** 4775–4785

20. Lee, S. H., Dobrzyn, A., Dobrzyn, P., Rahman, S. M., Miyazaki, M., and Ntambi, J. M. (2004) *J. Lipid Res.* **45,** 1674–1682

21. Althage, M. C., Ford, E. L., Wang, S., Tso, P., Polonsky, K. S., and Wice, B. M. (2008) *J. Biol. Chem.* **283,** 18365–18376

22. Folch, J., Lees, M., and Sloane Stanley, G. H. (1957) *J. Biol. Chem.* **226,** 497–509

23. Sampath, H., Miyazaki, M., Dobrzyn, A., and Ntambi, J. M. (2007) *J. Biol. Chem.* **282,** 2483–2493

24. Miyazaki, M., Dobrzyn, A., Elias, P. M., and Ntambi, J. M. (2005) *Proc. Natl. Acad. Sci. U.S.A.* **102,** 12501–12506

25. Shimomura, I., Bashmakov, Y., and Horton, J. D. (1999) *J. Biol. Chem.* **274,** 30028–30032

26. Miyazaki, M., Jacobson, M. J., Man, W. C., Cohen, P., Asilmaz, E., Friedman, J. M., and Ntambi, J. M. (2003) *J. Biol. Chem.* **278,** 33904–33911

27. Braun, K. M., Niemann, C., Jensen, U. B., Sundberg, J. P., Silva-Vargas, V., and Watt, F. M. (2003) *Development* **130,** 5241–5255

28. Lo Celso, C., Berta, M. A., Braun, K. M., Frye, M., Lyle, S., Zouboulis, C. C., and Watt, F. M. (2008) *Stem Cells* **26,** 1241–1252

29. Zheng, Y., Prouty, S. M., Harmon, A., Sundberg, J. P., Stenn, K. S., and Parimoo, S. (2001) *Genomics* **71,** 182–191

30. Payne, A. P. (1994) *J. Anat.* **185,** 1–49

31. Hillenius, W. J., Phillips, D. A., and Rehorek, S. J. (2007) *Ann. Anat.* **189,** 423–433

32. Miyazaki, M., Kim, H. J., Man, W. C., and Ntambi, J. M. (2001) *J. Biol. Chem.* **276,** 39455–39461

33. Horton, J. D., Goldstein, J. L., and Brown, M. S. (2002) *J. Clin. Invest.* **109,** 1125–1131

34. Fleury, C., Neverova, M., Collins, S., Raimbault, S., Champigny, O., Levi-Meyrueis, C., Bouillaud, F., Seldin, M. F., Surwit, R. S., Ricquier, D., and Warden, C. H. (1997) *Nat. Genet.* **15,** 269–272

35. Li, B., Nolte, L. A., Ju, J. S., Han, D. H., Coleman, T., Holloszy, J. O., and Semenkovich, C. F. (2000) *Nat. Med.* **6,** 1115–1120

36. Han, D. H., Nolte, L. A., Ju, J. S., Coleman, T., Holloszy, J. O., and Semenkovich, C. F. (2004) *Am. J. Physiol. Endocrinol. Metab.* **286,** E347–353

37. Neschen, S., Katterle, Y., Richter, J., Augustin, R., Scherneck, S., Mirhashemi, F., Schürmann, A., Joost, H. G., and Klaus, S. (2008) *Physiol. Genomics* **33,** 333–340

38. Clapham, J. C., Arch, J. R., Chapman, H., Haynes, A., Lister, C., Moore, G. B., Piercy, V., Carter, S. A., Lehner, I., Smith, S. A., Beeley, L. J., Godden, R. J., Herrity, N., Skehel, M., Changani, K. K., Hockings, P. D., Reid, D. G., Squires, S. M., Hatcher, J., Trail, B., Latcham, J., Rastan, S., Harper, A. J., Cadenas, S., Buckingham, J. A., Brand, M. D., and Abuin, A. (2000) *Nature* **406,** 415–418

39. Harper, M. E., Green, K., and Brand, M. D. (2008) *Annu. Rev. Nutr.* **28,** 13–33

40. Son, C., Hosoda, K., Ishihara, K., Bevilacqua, L., Masuzaki, H., Fushiki, T., Harper, M. E., and Nakao, K. (2004) *Diabetologia* **47,** 47–54

41. Wu, Z., Puigserver, P., Andersson, U., Zhang, C., Adelmant, G., Mootha, V., Troy, A., Cinti, S., Lowell, B., Scarpulla, R. C., and Spiegelman, B. M. (1999) *Cell* **98,** 115–124

42. Mead, J. R., Irvine, S. A., and Ramji, D. P. (2002) *J. Mol. Med.* **80,** 753–769

43. Kalaany, N. Y., Gauthier, K. C., Zavacki, A. M., Mammen, P. P., Kitazume, T., Peterson, J. A., Horton, J. D., Garry, D. J., Bianco, A. C., and Mangelsdorf, D. J. (2005) *Cell Metab.* **1,** 231–244

44. Narvaez, C. J., Matthews, D., Broun, E., Chan, M., and Welsh, J. (2009) *Endocrinology* **150,** 651–661

45. Ström, K., Hansson, O., Lucas, S., Nevsten, P., Fernandez, C., Klint, C., Movérare-Skrtic, S., Sundler, F., Ohlsson, C., and Holm, C. (2008) *PLoS ONE* **3,** e1793

46. Uldry, M., Yang, W., St-Pierre, J., Lin, J., Seale, P., and Spiegelman, B. M. (2006) *Cell Metab.* **3,** 333–341

47. Seale, P., Kajimura, S., Yang, W., Chin, S., Rohas, L. M., Uldry, M., Tavernier, G., Langin, D., and Spiegelman, B. M. (2007) *Cell Metab.* **6,** 38–54

48. Vidal-Puig, A., Solanes, G., Grujic, D., Flier, J. S., and Lowell, B. B. (1997) *Biochem. Biophys. Res. Commun.* **235,** 79–82

49. Vidal-Puig, A. J., Grujic, D., Zhang, C. Y., Hagen, T., Boss, O., Ido, Y., Szczepanik, A., Wade, J., Mootha, V., Cortright, R., Muoio, D. M., and Lowell, B. B. (2000) *J. Biol. Chem.* **275,** 16258–16266

50. Lowell, B. B., and Spiegelman, B. M. (2000) *Nature* **404,** 652–660

51. Puigserver, P., Wu, Z., Park, C. W., Graves, R., Wright, M., and Spiegelman, B. M. (1998) *Cell* **92,** 829–839

52. de Jesus, L. A., Carvalho, S. D., Ribeiro, M. O., Schneider, M., Kim, S. W., Harney, J. W., Larsen, P. R., and Bianco, A. C. (2001) *J. Clin. Invest.* **108,** 1379–1385

53. Kim, B. (2008) *Thyroid* **18,** 141–144

54. Gereben, B., Zeöld, A., Dentice, M., Salvatore, D., and Bianco, A. C. (2008) *Cell. Mol. Life Sci.* **65,** 570–590

55. Pelletier, P., Gauthier, K., Sideleva, O., Samarut, J., and Silva, J. E. (2008) *Endocrinology* **149,** 6471–6486

56. Watanabe, M., Houten, S. M., Mataki, C., Christoffolete, M. A., Kim, B. W., Sato, H., Messaddeq, N., Harney, J. W., Ezaki, O., Kodama, T., Schoonjans, K., Bianco, A. C., and Auwerx, J. (2006) *Nature* **439,** 484–489

57. Wondisford, F. E. (2006) *Cell Metab.* **3,** 81–82

58. Ukropec, J., Anunciado, R. P., Ravussin, Y., Hulver, M. W., and Kozak, L. P. (2006) *J. Biol. Chem.* **281,** 31894–31908

59. Elias, P. M., and Feingold, K. R. (1992) *Semin. Dermatol.* **11,** 176–182

60. Smith, K. R., and Thiboutot, D. M. (2008) *J. Lipid Res.* **49,** 271–281

61. Fluhr, J. W., Mao-Qiang, M., Brown, B. E., Wertz, P. W., Crumrine, D., Sundberg, J. P., Feingold, K. R., and Elias, P. M. (2003) *J. Invest. Dermatol.* **120,** 728–737

62. Lu, Y., Bu, L., Zhou, S., Jin, M., Sundberg, J. P., Jiang, H., Qian, M., Shi, Y., Zhao, G., Kong, X., and Hu, L. (2004) *Mol. Genet. Genomics* **272,** 129–137

63. Binczek, E., Jenke, B., Holz, B., Günter, R. H., Thevis, M., and Stoffel, W. (2007) *Biol. Chem.* **388,** 405–418

64. Jong, M. C., Gijbels, M. J., Dahlmans, V. E., Gorp, P. J., Koopman, S. J., Ponec, M., Hofker, M. H., and Havekes, L. M. (1998) *J. Clin. Invest.* **101,** 145–152

65. Yagyu, H., Kitamine, T., Osuga, J., Tozawa, R., Chen, Z., Kaji, Y., Oka, T., Perrey, S., Tamura, Y., Ohashi, K., Okazaki, H., Yahagi, N., Shionoiri, F., Iizuka, Y., Harada, K., Shimano, H., Yamashita, H., Gotoda, T., Yamada, N., and Ishibashi, S. (2000) *J. Biol. Chem.* **275,** 21324–21330

66. Karnik, P., Tekeste, Z., McCormick, T. S., Gilliam, A. C., Price, V. H., Cooper, K. D., and Mirmirani, P. (2009) *J. Invest. Dermatol.* **129,** 1243–1257

67. Michalik, L., and Wahli, W. (2007) *Biochim. Biophys. Acta* **1771,** 991–998

68. Shih, M. Y., Kane, M. A., Zhou, P., Streeper, R. S., Yen, C. L., Napoli, J. L., and Farese, R. V., Jr. (2009) *J. Biol. Chem.* **284,** 4292–4299

69. Mirza, R., Hayasaka, S., Takagishi, Y., Kambe, F., Ohmori, S., Maki, K., Yamamoto, M., Murakami, K., Kaji, T., Zadworny, D., Murata, Y., and Seo, H. (2006) *J. Invest. Dermatol.* **126,** 638–647

70. Overton, J. M., and Williams, T. D. (2004) *Physiol. Behav.* **81,** 749–754

71. Feldmann, H. M., Golozoubova, V., Cannon, B., and Nedergaard, J. (2009) *Cell Metab.* **9,** 203–209

72. Lodhi, I. J., and Semenkovich, C. F. (2009) *Cell Metab.* **9,** 111–112

73. Silva, J. E. (2006) *Physiol. Rev.* **86,** 435–464

74. Jensen, D. R., Knaub, L. A., Konhilas, J. P., Leinwand, L. A., MacLean, P. S., and Eckel, R. H. (2008) *J. Lipid Res.* **49,** 870–879

75. Rousset, S., Alves-Guerra, M. C., Mozo, J., Miroux, B., Cassard-Doulcier, A. M., Bouillaud, F., and Ricquier, D. (2004) *Diabetes* **53,** Suppl. 1, 130–135

76. Liu, X., Rossmeisl, M., McClaine, J., Riachi, M., Harper, M. E., and Kozak, L. P. (2003) *J. Clin. Invest.* **111,** 399–407
77. Chen, H. C., Smith, S. J., Tow, B., Elias, P. M., and Farese, R. V., Jr. (2002) *J. Clin. Invest.* **109,** 175–181
78. Smith, S. J., Cases, S., Jensen, D. R., Chen, H. C., Sande, E., Tow, B., Sanan, D. A., Raber, J., Eckel, R. H., and Farese, R. V., Jr. (2000) *Nat. Genet.* **25,** 87–90
79. Jong, M. C., Voshol, P. J., Muurling, M., Dahlmans, V. E., Romijn, J. A., Pijl, H., and Havekes, L. M. (2001) *Diabetes* **50,** 2779–2785
80. Xie, Z., Komuves, L., Yu, Q. C., Elalieh, H., Ng, D. C., Leary, C., Chang, S., Crumrine, D., Yoshizawa, T., Kato, S., and Bikle, D. D. (2002) *J. Invest. Dermatol.* **118,** 11–16
81. Rodgers, J. T., Lerin, C., Gerhart-Hines, Z., and Puigserver, P. (2008) *FEBS Lett.* **582,** 46–53